NIPPON STEEL TECHNICAL REPORT No. 57 APRIL 1993

UDC620.192.43/.45

Mathematical Analysis of Segregation and Compositional Changes of Nonmetallic Inclusions in Steel during Solidification

Tooru Matsumiya*1 Wataru Yamada*1
Toshihiko Koseki*1 Yoshiyuki Ueshima*1

Abstract:

Here are described a method for analyzing microsegregation in steel during solidification by the finite element method; a coupled precipitation model for analyzing the compositional changes of nonmetallic inclusions in the solidification process; a method for applying the phase diagram simulation technique to the analysis of equilibrium between liquid steel and nonmetallic inclusions; and a method for solving the solute diffusion by the finite element method and applying a model of transformation following equilibrium in each element or transformation according to kinetics. The results obtained from the application of these methods to the analysis of spot-like segregation, sulfide shape control in hydrogen induced cracking (HIC)-resistant steel, nonmetallic inclusions in stainless steel, and volume fraction of the residual δ phase in stainless steel welds are discussed in comparison with experimental results.

1. Introduction

Nonmetallic inclusions in steel often deteriorate the mechanical properties of the steel. Much effort is made to reduce the amount of nonmetallic inclusions in continuously cast steel by encouraging their flotation and separation through the control of liquid steel flow in the tundish and mold. Since fine nonmetallic inclusions cannot be totally removed, it is equally important to control their chemical composition so as to render them harmless to steel processing and quality of end products.

When manganese sulfide precipitates in the center line segregation of a continuously cast slab of the hydrogen induced cracking (HIC)-resistant steel to be described later, it remains as an elongated film amid the wall thickness of line pipe, the end product, and causes HIC in the pipe. Calcium is added to prevent this precipitation of MnS[1-3]. When hard nonmetallic inclusions are present in the steel for tire cords, they cause wire breakage during drawing. For this steel grade, therefore, deoxidation conditions are selected so as to obtain easy-to-elongate and low-melting point nonmetallic inclusions[4,5]. In addition, the positive use of oxides in the structural control of steel is recently drawing renewed attention[6,7]. This makes it necessary to find out oxides that are effective for this purpose.

In the cases mentioned above, nonmetallic inclusions left in steel undergo the steel solidification process. It is important to analyze compositional changes in the nonmetallic inclusions, including the influences of solidification segregation.

Center line segregation results from the flow of residual liquid steel between dendrites. The residual δ phase volume fraction that governs the mechanical properties of stainless steel welds is also strongly affected by interdendritic microsegregation. All this adds to the importance of analyzing the solidification microsegregation. Microsegregation must be correctly grasped also from the viewpoint of analyzing the compositional change

*1 Technical Development Bureau

of nonmetallic inclusions in the steel solidification process. From the above standpoint, the authors conducted a series of mathematical analyses on the relevant subjects.

2. Mathematical Analysis of Solidification Microsegregation

Solidification microsegregation has been traditionally analyzed for three cases: where the entire system of the solid phase and liquid phase is assumed to be in thermodynamic equilibrium; where the solutes are assumed to be completely mixed in the liquid phase and the solute diffusion in the solid phase is totally ignored; and where the solutes are assumed to be completely mixed in the liquid phase and to be diffused in the solid phase, although to a small degree. An equation is derived to describe the relationship between the solid fraction f_S and the solute concentration C_L in each case as follows:

$$C_L = C_0/\{1-(1-k)\ f_s\} \quad \cdots\cdots(1)$$

$$C_L = C_0(1-f_s)^{k-1} \quad \cdots\cdots(2)$$

$$C_L = C_0\{1-(1-2\alpha k)\ f_s\}^{(k-1)/(1-2\alpha k)} \quad \cdots\cdots(3)$$

where C_0 is the average solute concentration, and k is the equilibrium partition coefficient between the solid and liquid phases. Equations (1) to (3) are called the equation for equilibrium solidification, the Scheil equation[8], and the Brody-Flemings equation[9], respectively. α is a solidification parameter defined as $\alpha = 4D \cdot t_S/L^2$, where D is the solute diffusion coefficient in the solid phase, t_S is the local solidification time, and L is the dendrite arm spacing.

Clyne and Kurz indicated that a problem occurs in Eq. (3) as the solute diffusion in the solid phase becomes conspicuous and assumes a large value. They proposed Eq. (5) where Ω defined by Eq. (4) is used in Eq. (3) in place of α[10].

$$\Omega = \alpha\{1-\exp(-1/\alpha)\} - 1/2 \cdot \exp(-1/2\alpha) \quad \cdots\cdots(4)$$

$$C_L = C_0\{1-(1-2\Omega k) f_s\}^{(k-1)/(1-2\Omega k)} \quad \cdots\cdots(5)$$

Equation (5) agrees with Eq. (1) when the solute diffusion in the solid phase becomes noticeable, and agrees with Eqs. (3) and (2) when the solute diffusion in the solid phase is limited. In other words, Eq. (5) provides a qualitatively reasonable description of segregation. However, the rate at which Eq. (5) approaches Eq. (1) or Eqs. (3) and (2) is quantitatively ambiguous.

The above ambiguity was eliminated by applying the finite difference method (FDM) to the analysis of microsegregation[11]. As shown in **Fig. 1**, the transverse section of a growing dendrite was divided into finite elements, and the solute diffusion normal to the dendrite axis was analyzed. The temperature T_A of the analysis region was assumed to be already given, and a method was devised whereby the solid/liquid interface was assumed to advance following the temperature change while maintaining a thermodynamic equilibrium.

More specifically, the solid/liquid interface is instantaneously advanced by one element when the liquidus temperature T_L calculated from the solute concentration in the N-th element (liquid at the solid/liquid interface) in **Fig. 2** agrees with T_A. The solute concentrations in the N-th and (N+1)-th elements just after the advancement of the solid/liquid interface are determined by assuming that the sum of the solute content of the N-th element and that of the (N+1)-th element is conserved, and that the solute concentration ratio of the solid N-th element to the liquid (N+1)-th element is kept at the solid/liquid equilibrium partition coefficient k. Since the solute concentration in the (N+1)-th element concomitantly becomes higher, the value of T_L thus calculated becomes lower than T_A.

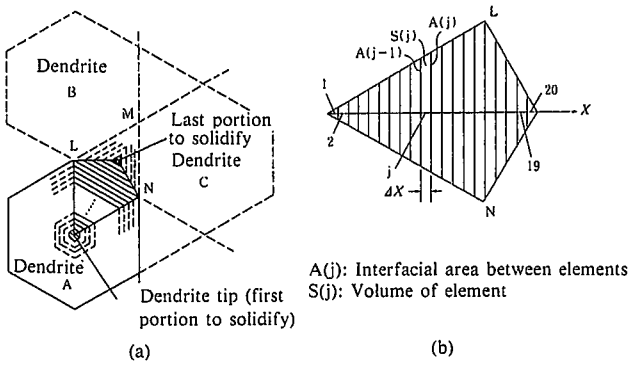

Fig. 1 Schematic illustration of dendrite transverse section (a) and element division of segregation calculation region (b)[11]

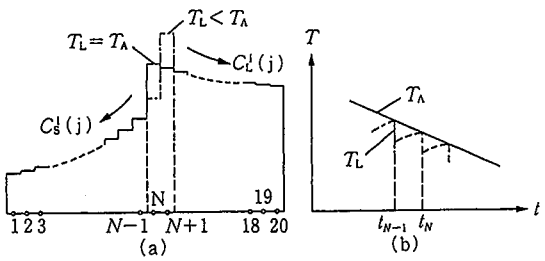

(a) solid line: when (N−1)-th element completely solidified
dot-dash line: when N-th element subsequently solidified immediately

(b) solid curve: Actual temperature given
dashed curve: Liquidus temperature calculated from solute concentration in liquid phase at solid/liquid interface

$C_L^i(j)$: Concentration of solute element i in element j in liquid phase
$C_S^i(j)$: Concentration of solute element i in element j in solid phase
t: Time

Fig. 2 Schematic illustration of segregation calculation by finite difference method: (a) solute distribution in each element; (b) relationship between preset temperature T_A and liquidus temperature T_L calculated from solute concentration in liquid phase at solid/liquid interface[11]

The process of the concentrated solutes diffusing from the solid/liquid interface into both the solid and liquid phases was analyzed by the FDM technique with the solid/liquid interface fixed in location. The solute concentration ratio of the N-th element to the (N+1)-th element was kept at k in the process, or, in other words, the N-th and (N+1)-th elements were assumed to be in equilibrium. The solute diffusion decreases the solute concentration in the (N+1)-th element with time and increases the value of T_L calculated from the solute concentration. Since T_A decreases with time, on the other hand, T_L becomes equal to T_A at some point of time. At this point, the solid/liquid interface is advanced by another element. This procedure can be repeated to analyze microsegregation by advancing the solid/liquid interface while approximately satisfying $T_L = T_A$.

It was established that the results of microsegregation calculated by this method agree with those calculated by the above-mentioned simple microsegregation equations under the conditions where the equations are applicable and that this method can provide results in accord with the measurement of segregation and solidification time in unidirectional solidification experi-

ments and the observation of spot-like segregation in continuously cast slabs (see **Figs. 3** and **4**). The authors extended this method to cover the δ/γ interface as well as the solid/liquid interface[12] and used it in analyzing the effects of many alloying elements on microsegregation in alloy systems that undergo the δ-γ transformation[13].

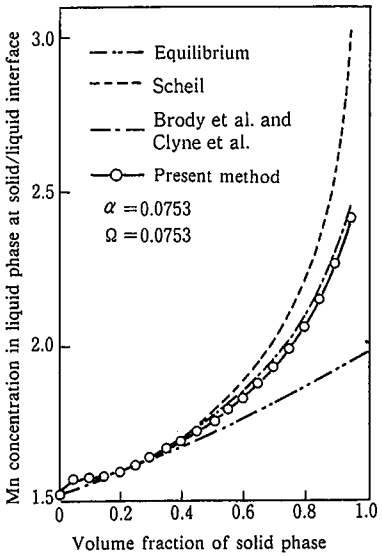

Fig. 3 Comparison of results of microsegregation calculation by conventional equations and results of microsegregation calculation by new method[11]

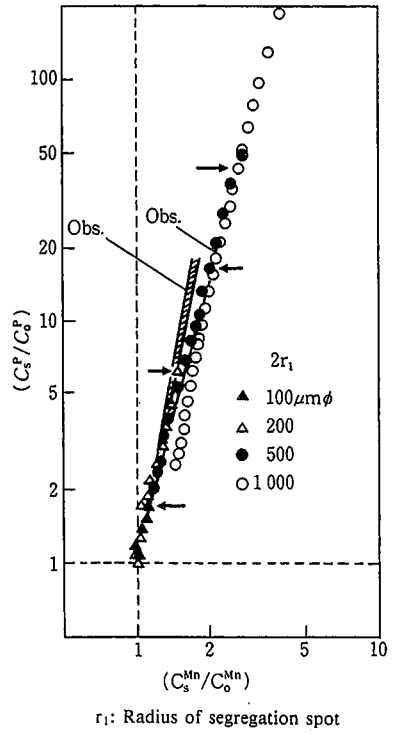

r_1: Radius of segregation spot

Fig. 4 Comparison of calculated and measured values of Mn concentration C_S^{Mn} and P concentration C_S^P in spot-like segregation in HIC-resistant steel[11]

3. Mathematical Analysis of Compositional Changes in Nonmetallic Inclusions

3.1 Coupled precipitation model

Compositional changes in and the precipitation and annihilation of nonmetallic inclusions in residual liquid steel were analyzed following the process of deriving Eqs. (3) and (5), while giving consideration to solidification segregation (see **Fig. 5**)[14]. The following assumptions were made:

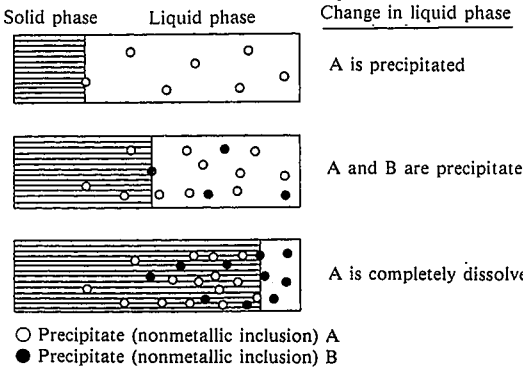

Fig. 5 Schematic illustration of coupled precipitation model in solidification process[14]

1) The solid/liquid interface is in local equilibrium.
2) Solutes in the liquid phase are completely mixed and in equilibrium with uniformly distributed nonmetallic inclusions.
3) The solute diffusion in the solid phase is modeled according to Clyne and Kurz.
4) Nonmetallic inclusions are not rejected at the solid/liquid interface but are sequentially incorporated into the solid phase.
5) Reactions in the solid phase are ignored.

The following equation is derived from the above assumptions:

$$(1-k^i)\, C_L^i\, df_s = \{1-(1-2\Omega^i)\, k^i f_s\}\, dC_L^i + (1-f_s) \sum_j R_{ij} dP_j \quad \cdots\cdots(6)$$

where the superscript i indicates the value of a solute i; P_j is the molar fraction of a component compound existing as a nonmetallic inclusion; and R_{ij} is the number of moles or stoichiometric number of the solute i contained in 1 mol of the component compound j. The left side of Eq. (6) indicates the amount of the solute i rejected from the solid/liquid interface, a part of which is used in the solute diffusion $2\Omega^i k^i f_S dC_L^i$ in the solid phase. The rest of the rejected solute i is used in the increment dP_j in the nonmetallic inclusions in the residual liquid steel by $(1-f_S)\sum_j R_{ij} dP_j$ and in the increment dC_L^i in the amount of the solute i dissolved in the liquid phase by $(1-f_S)dC_L^i$. Equation (6) indicates the balance among these amounts of the solute i. If $P_j = 0$ in Eq. (6), $dP_j = 0$. The last term is eliminated, and integration yields Eq. (5).

If $P_j \neq 0$, another unknown quantity dP_j is added. The equation of equilibrium or Eq. (7) holds because of the assumption 2) above, and Eq. (8) is obtained as a derivative form of Eq. (7). The two equations are simultaneously solved to obtain the relations of dC_L^i and dP_j with df_s. Integration of these relations leads to C_L^i and P_j each as a function of f_S.

$$\prod_i a_i^{R_{ij}} = K_j a_j \quad \cdots\cdots(7)$$

$$\sum_i R_{ij}\, da_i/a_i = dK_j/K_j + da_j/a_j \quad \cdots\cdots(8)$$

where a_i is the activity of the solute i in the residual liquid steel; K_j is the reaction equilibrium constant of the compound j calculated from the standard free energy of formation; and a_j is the activity of the compound j. a_i is expressed as a function of C_L^i, and a_j is expressed as a function of P_j. K_j is a function of temperature and also is a function of C_L^i because the temperature is the liquidus temperature T_L according to assumption 1) and is related to C_L^i. Equation (8) thus gives a new relation between dC_L^i and dP_j.

This analytical model is named the coupled precipitation model because it can analyze the way the various compounds grow or redissolve in equilibrium coupled with the liquid steel through the solutes segregated into the residual liquid between dendrites.

Methods have been proposed for balancing calcium with other alloying elements to perform sulfide shape control as an effective measure for preventing the hydrogen induced cracking (HIC) of line pipe steel for sour service[1-3]. These methods, however, do not precisely consider the change in the shape of nonmetallic inclusions in the solidification process, as pointed out in the analysis by Kitamura et al.[15]. Using the coupled precipitation model, therefore, the compositional change of nonmetallic inclusions during solidification was analyzed for spot-like segregation in HIC-resistant steel slabs.

Spot-like segregation is believed to form when the residual liquid steel between dendrites as solidified to an advanced degree are squeezed out by solidification contraction or bulging and are entrapped in the thickness center of the slab. The spot-like segregation calculated by assuming that the residual liquid steel was rejected out of dendrites when the volume fraction of the solidified dendrites was 90% agreed well with the spot-like segregation observed in actual slabs[11]. This finding was used also in the analysis of nonmetallic inclusions.

Table 1 shows the average chemical composition of the steel in question and the C_L^{90}, composition of residual liquid steel between dendrites when $f_S = 0.9$. The C_L^{90} composition was calculated by Eq. (5). $L = 200\ \mu m$ and $t_S = 200$ s, which correspond to the secondary arm spacing and local solidification time in the center of the continuously cast slab, respectively, were used as conditions. The relations between the solid fraction f_S, the solute concentration C_L^i in the residual liquid steel, and the content P_j of the compound j as nonmetallic inclusion during the solidification of the spot-like segregation of the C_L^{90} composition were calculated by Eqs. (6) and (8). The diameter of the spot-like segregation was used as L, and t_S was 200 s. The dissolution of the solute elements C, Si, Mn, P, S, Al, Ca and O and the precipitation of CaO, Al_2O_3, MnS and CaS were taken into consideration. The activities of CaO and Al_2O_3, a_{CaO} and $a_{Al_2O_3}$ were considered to be dependent on the composition of the CaO-Al_2O_3 compound. The activities of MnS and CaS were taken as unity when they precipitated. The compound j was judged to have precipitated when the product of the activities of dissolved solutes reached the value of the right side of Eq. (7) and was judged to have been annihilated when $P_j = 0$ because the calculation was performed while satisfying Eq. (7) as far as P_j was considered.

Table 1 Average chemical compostion of HIC-resistant steel and calculated concentrations of solute elements in residual liquid steel between dendrites at 90% solid fraction[14]

(mass%)

	C	Si	Mn	P	S	Al	Ca	O
Average	0.081	0.16	1.02	0.0050	0.0012	0.0290	0.0033	0.0025
C_L^{90}	0.317	0.218	1.32	0.0203	0.0090	0.0447	0.0270	0.0270

The results of calculation for $L = 100\ \mu m$ are as shown in **Figs. 6(a)** and **(b)**. P_j is expressed in the unit of the mass percentage of oxygen existing as an oxide when the compound j is the oxide and the mass percentage of sulfur existing as a sulfide when the compound j is the sulfide. The calculated values indicate that at the start of solidification of the spot-like segregation, oxygen is mostly fixed as $12CaO \cdot 7Al_2O_3$ (abbreviated $C_{12}A_7$ with other complex compounds shown in a similarly abbreviated form), and C_L^O is less than 1 ppm. Some of the calcium is expended to fix oxygen as $C_{12}A_7$, and the rest of the calcium is mostly consumed to fix sulfur as CaS. C_L^{Ca} is about 0.01 ppm.

As solidification proceeds further, CaO in the CaO-Al_2O_3 compound decomposes, calcium fixes the segregating sulfur as

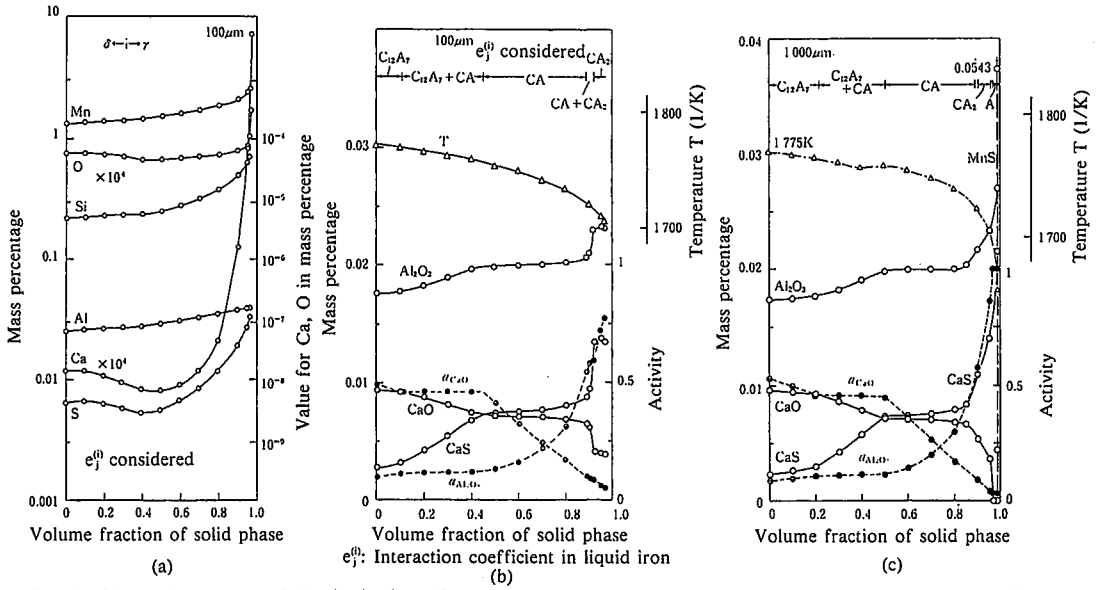

Fig. 6 Changes in amounts of dissolved solutes (L = 100 μm) (a), of nonmetallic inclusions (L = 100 μm) (b), and of nonmetallic inclusions (L = 1,000 μm) (c) in residual liquid steel in spot-like segregation during solidification[14]

CaS, P_{CaS} increases, oxygen is fixed by aluminum, and the Al_2O_3 content of the CaO-Al_2O_3 compound increases. In this case, CaO is not completely decomposed until the completion of the solidification, the sulfur segregating to the last is fixed as CaS, and the precipitation of MnS is suppressed. **Fig. 6 (c)** gives the results of calculation for the same chemical composition but for L = 1000 μm. The curves change mostly in the same way as shown for L = 100 μm, but CaO is completely decomposed and annihilated at f_S = 0.98. The only calcium source required to fix the segregating sulfur thereafter is the one dissolved in trace amounts. Consequently, MnS precipitates toward the end of the solidification process.

The above results of calculation are compared with the spot-like segregation observed in continuously cast slabs. Arihara et al. estimated the solidification sequence of spot-like segregation by using the isoconcentration lines of manganese (the higher the manganese concentration, the higher the volume fraction f_S of the solid phase), and investigated the distribution of various compounds with respect to f_S[16]. According to their findings, CaO is largely distributed in the first half of the solidification process, CaS is largely distributed in the last half of the solidification process, and MnS is present only in the last portion to solidify. These tendencies agree with the results of calculation shown in **Fig. 6**.

Fukuda et al. defined as spot-like segregation a portion with a manganese concentration over 1.32 times the average value (approximately the same as C_L^{90} of manganese in the bottom row of **Table 1**), investigated the relationship between the segregation diameter and the maximum manganese concentration, found that the maximum manganese concentration suddenly increases as the segregation diameter exceeds about 270 μm (see **Fig. 7**), and cited the precipitation of MnS as the cause of the sudden increase[16]. For comparison with these results, computation was performed for the values of L other than 100 and 1,000 μm. It was consequently clarified that when L exceeds 300 μm, MnS starts to precipitate at the residual liquid phase volume fraction of about 1%. The calculated results are in good agreement with the measured results.

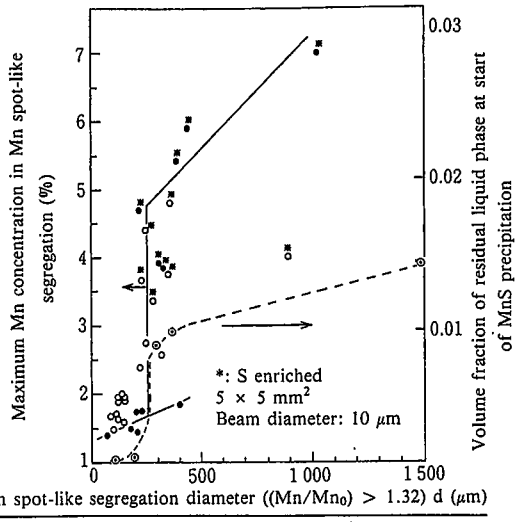

Fig. 7 Relationship between diameter of spot-like segregation, maximum Mn concentration (measured) in spot-like segregation[16], and volume fraction of residual liquid phase (calculated) at start of MnS precipitation[14]

3.2 Model adopting phase diagram simulation method

The above-mentioned coupled precipitation model is a universal model that can handle the precipitation of all solutes and compounds in principle. On the other hand, in the field of computer simulation of phase diagrams (CALPHAD for CALculation of PHAse Diagram), very versatile methods have been developed for the calculation of thermodynamic equilibrium[17,18]. Thermodynamic data bases[19] and integrated systems of phase diagram simulation[20] have also been developed. The authors carried out the development of more versatile methods utilizing these past achievements.

The authors first developed a method for analyzing carbon steel through the application of Solgasmix (a thermodynamic equilibrium computation program)[18], analyzed precipitates in spot-like segregation in HIC-resistant steel by the analytical method, and indicated that the results of calculation by the coupled precipitation model can be reproduced by the analytical method[21]. We then developed jointly with Sundman, who developed Thermo-Calc (a phase diagram computation program)[20], a more generalized method that can be applied to high-alloy steels like stainless steel[22]. Still another method was devised for discretely solving Eq. (5) using Thermo-Calc. First, the solid phase is precipitated in a trace amount by lowering the preset temperature for equilibrium calculation by a small degree. Then, the solid phase is discarded out of the system, and another equilibrium calculation is performed on the residual liquid phase by lowering the preset temperature. The solid phase is again precipitated in a trace amount and discarded out of the system. This procedure is repeated to discretely solve the Scheil equation, or Eq. (2).

Before incorpo rating the effect of the solute diffusion in the solid phase, differential forms of Eqs. (2) and (5) are compared.

$$(1-k)C_L df_s - (1-f_s)dC_L \quad \cdots\cdots(2')$$

$$(1-k)C_L df_s = (1-f_s)dC_L + 2\Omega k f_s dC_L \quad \cdots\cdots(5')$$

The two equations are the same on the left side (amount of solute rejected with progress of solidification). Equation (5') has on the right side the surplus term $2\Omega k f_S dC_L$ that indicates the amount of the solutes consumed by their diffusion in the solid phase. According to Eq. (2), dC_L can be discretely obtained by taking the difference in C_L between the previous step and the present step of the above-mentioned procedure. If $\Delta C_{L,Sc}$ is the value thus determined and $\Delta C_{L,C\text{-}K}$ is the increment according to Eq. (5), the ratio of the two values is obtained from Eqs. (2') and (5') as given by

$$\Delta C_{L,\,C\text{-}K} = (1-f_s)/\{(1-f_s)+2\Omega f_s k\}\ \Delta C_{L,\,Sc} \quad \cdots\cdots(9)$$

Therefore, $\Delta C_{L,C\text{-}K}$ can be obtained from $\Delta C_{L,Sc}$. More specifically, a given temperature is set, the equilibrium at the preset temperature is calculated, the precipitation of the matrix solid phase and nonmetallic inclusions is calculated, the increment of C_L from the previous step is expressed by $\Delta C_{L,Sc}$ and modified to $\Delta C_{L,C\text{-}K}$ by incorporating the compensation for the solute diffusion in the solid phase using Eq. (9), and C_L at the present step is corrected by $\Delta C_{L,C\text{-}K}$ in place of $\Delta C_{L,S}$.

Nonmetallic inclusions are assumed to be uniformly distributed in the newly precipitated solid phase and the liquid phase, and the solute composition of the liquid phase is determined from the sum of the nonmetallic inclusions distributed in the liquid

phase and C_L. In the next step, the solid phase is separated, the equilibrium is calculated for the liquid phase at a slightly lower temperature, and the precipitation of the matrix solid phase and nonmetallic inclusions and the distribution of the dissolved solutes are calculated again. This procedure is repeated in subsequent steps. From the increment Δf_S in the volume fraction of the solid phase and the drop ΔT in the preset temperature respectively from the preceding step, the value of t_S at each point in time is calculated as $t_S = \Delta T/(R \cdot \Delta f_S)$ according to the cooling rate R and is reflected in the calculation of α and Ω.

This method was used to analyze the changes in C_L^i and P_j in the solidification process of 21%Cr-11%Ni stainless steel (0.1%Si-0.002%Al-0.002%Ca-0.005%O, each in mass percent). The results are shown in **Fig. 8**, where L is 100 μm and t_S is 100 s. The precipitation of Cr_2O_3 was also analyzed in detail. The method is being utilized in controlling the nonmetallic inclusions in stainless steels.

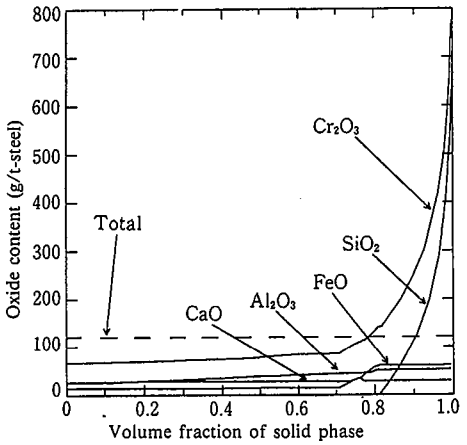

Fig. 8 Changes in contents of compounds in nonmetallic inclusions in residual liquid phase in solidification process as calculated through combination with Thermo-Calc

4. Analysis by Finite Difference Method and Thermodynamic Equilibrium Calculation Method Combined

The authors analyzed the solidification of stainless steel weld pools[23]. The transverse section of a growing dendrite is divided into elements as shown in **Figs. 1** and **2**, the solute diffusion between the elements is analyzed by the finite difference method (FDM), and the thermodynamic equilibrium in each element is calculated on the basis of the solute balance. This method accurately analyzed the movement of the solid/liquid interface and the distribution of solutes. The thermodynamic equilibrium did not always hold in each element during the δ-γ transformation at temperatures under 1,473 K. The Clyne-Kurz equation, or Eq. (5), was applied to the δ-γ transformation. The solutes were assumed to be completely mixed within the δ phase in each element, and the solute diffusion in the γ phase was partly taken into consideration. The solute diffusion between the elements was calculated by the FDM technique. The solute diffusion through the γ phase between the elements was negligibly small.

Fig. 9 shows the distributions of nickel and chromium on the transverse section of growing dendrite as an example of analyzed results. The calculated results agree well with the results observed

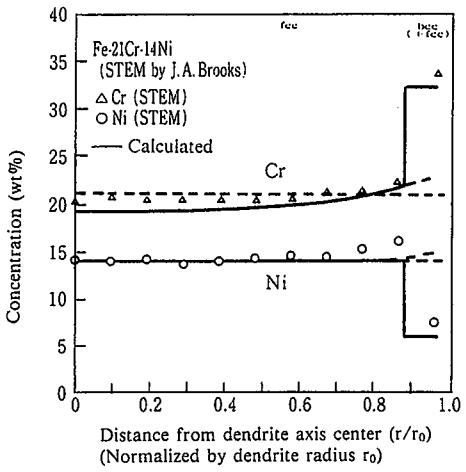

Fig. 9 Comparison of calculated solute concentrations[23] and STEM measured solute concentrations[24] in stainless steel weld pools

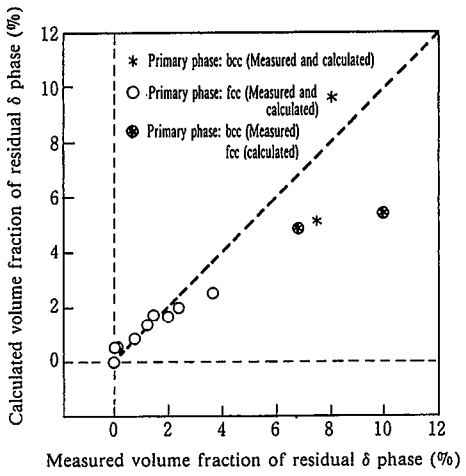

Fig. 10 Comparison of calculated and measured volume fractions of residual δ phase in stainless steel welds[23]

by Brooks and et al. under the scanning transmission electron microscope (STEM)[24]. **Fig. 10** compares the calculated and measures values of the volume fraction of residual δ phase. As seen, the calculated values are in fairly good accord with the measured values.

5. Conclusions

A method was developed for analyzing solidification microsegregation using the finite difference method (FDM), and was applied to the analysis of microsegregation and spot-like segregation. The values calculated by the method agreed well with measured values. As a technique for analyzing the compositional changes of nonmetallic inclusions in the solidification process, a coupled precipitation model was developed adopting the Clyne-Kurz treatment of microsegregation and assuming that nonmetallic inclusions in the residual liquid steel change while maintaining thermodynamic equilibrium with the liquid steel. The model was applied to the sulfide shape control of hydrogen induced cracking-resistant steel and theoretically proved to reproduce the actual situation. The analytical method was generalized with the

aid of Solgasmix and Thermo-Calc, making it possible to analyze the compositional changes of nonmetallic inclusions in stainless steels.

Lastly, a method was proposed in which a solidification or transformation analysis region is divided into finite elements, a thermodynamic equilibrium is assumed in each element or a transformation kinetic model is applied, and transport equations between the elements are solved by the FDM approach. The method was applied to the analysis of the solidification and subsequent transformation phenomena in stainless steel weld pools, and was demonstrated to be capable of predicting the volume fraction of the residual δ phase.

References

1) Haida, O. et al.: Tetsu-to-Hagané. 64, 1538 (1978)
2) Nakasugi, H. et al.: Seitetsu Kenkyu. (297), 72 (1979)
3) Haida, O. et al.: Tetsu-to-Hagané. 66, 354 (1980)
4) Shiraiwa, T. et al.: The Sumitomo Search. (11), 85 (1974)
5) Okushima, N.: 126th and 127th Nishiyama Memorial Lecture, Tokyo, 1988, Iron Steel Inst. Jpn., p. 145
6) Takamura, J., Mizoguchi, S.: Proc. 6th Int. Iron and Steel Cong. Vol. 1, Iron Steel Inst. Jpn., 1990, p. 591
7) Mizoguchi, S., Takamura, J.: Proc. 6th Int. Iron and Steel Cong. Vol. 1, Iron Steel Inst. Jpn., 1990, p. 598
8) Scheil, E.: Z. Metallkd. 34, 70 (1942)
9) Brody, H.D., Flemings, M.C.: Trans. Metall. Soc. AIME. 236, 615 (1966)
10) Clyne, T.W., Kruz, W.: Metall. Trans. A. 12A, 965 (1981)
11) Matsumiya, T. et al.: Trans, Iron Steel Inst. Jpn. 24, 873 (1984)
12) Ueshima, Y. et al.: Metall. Trans. B. 17B, 845 (1986)
13) Ueshima, Y. et al.: Tetsu-to-Hagané. 73, 1551 (1987)
14) Matsumiya, T., Ohashi, T.: Tetsu-to-Hagané. 71, S1069 (1985)
15) Kitamura, S. et al.: Tetsu-to-Hagané. 73, 677 (1987)
16) Fukuda, Y. et al.: Tetsu-to-Hagané. 71, S218 (1985)
17) Hasebe, M., Nishizawa, T.: Bull. Jpn. Inst. Metals. 11, 879 (1972)
18) Eriksson, G.: Chemica Scripta. 8, 100 (1975)
19) Gallangher, R.G. et al.: Steel Res. 56, 7 (1985)
20) Sundman, B. et al.: CALPHAD. 9, 153 (1985)
21) Yamada, W. et al.: Proc. 6th Int. Iron Steel Cong. Vol. 1, Iron Steel Inst. Jpn., 1990, p. 618
22) Yamada, W. et al.: Computer Aided Innovation of New Materials. Amsterdam, North Holland, 1991, p. 587
23) Koseki, T. et al.: In preparation
24) Brooks, J.A. et al.: Metall. Trans.. A. 14A, 23 (1983)